A detailed investigation into the oxidation mechanism of Hantzsch 1,4-dihydropyridines by ethyl α-cyanocinnamates and benzylidenemalononitriles

Xiao-Qing Zhu,* Hong-Ling Zou, Ping-Wei Yuan, Yang Liu, Lei Cao and Jin-Pei Cheng*

Department of Chemistry, Nankai University, Tianjin 300071, China

Received (in Cambridge, UK) 27th April 2000, Accepted 6th July 2000
Published on the Web 14th August 2000

The mechanism for the oxidation of Hantzsch 1,4-dihydropyridine (HEH) by substituted ethyl α-cyanocinnamates (**1**) and benzylidenemalononitriles (**2**) has been critically investigated. Replacement of HEH by HEH-4,4-d_2 and HEH-*N*-d gave the observed kinetic isotope effects (KIE) of 5.3–6.0 and 1.2–1.3 for the reactions with **1** and **2**, respectively, which suggests C_4–H bond dissociation is involved in the rate-limiting step and that the N–H bond dissociation is a non-rate-limiting step. The positive ρ values of 1.78 and 1.67 for the reactions of HEH with **1** and **2**, respectively, clearly demonstrate the electrophilic nature of the substrates in the transition state (TS) and so indicate that the hydrogen lost from HEH must be a hydride-like species. Correlation analyses on the kinetics, KIE's, and activation parameters showed excellent linear dependence on the electronic properties of remote substituents and added further credence to the proposed one-step hydride transfer mechanism. Detailed investigation of the activation parameters not only confirmed the direct H_T^- mechanism, but also revealed experimentally, for the first time, an entropy-controlled compact TS for the HEH-modeled NAD(P)H oxidations.

Introduction

The reduced form of the nicotinamide adenine dinucleotide coenzyme [NAD(P)H] plays an important role in many bioreductions by transferring a hydride ion or an electron to the surrounding substrates.[1] The mechanism of reactions mediated by NAD(P)H and its models has been extensively studied[2,3] and continues to attract considerable attention because of the need to understand the finer details of the mechanism. Concerning the reaction mechanism one critical yet controversial issue is whether the formal hydride transfer from NAD(P)H and its model compounds to the substrates occurs by one-step direct detachment or by a multi-step sequential e^-–H^+–e^- process. Evidence has been reported in support of the e^-–H^+–e^- transfer mechanism for many thermal reactions in which strong oxidants are involved.[4] Evidence for the direct hydride transfer mechanism has also been reported in reactions with aldehydes and ketones, in particular, in the cases of most NAD(P)$^+$/NAD(P)H mediated enzymatic reactions.[5] In NAD(P)H mimic studies, the most frequently used model compounds are 1-benzyl-1,4-dihydronicotinamide (BNAH) and 10-methyl-9,10-dihydroacridine (AcrH$_2$).[6] Hantzsch esters, which are also known as very close analogues of NAD(P)H and possess a high biological activity as a class of calcium antagonists,[7] have scarcely been studied as NAD(P)H models in comparison to BNAH and AcrH$_2$. This lack of interest may have arisen from the fact that Hantzsch esters (HEH) have two hydrogen atoms (at the 1- and 4-positions) to lose in the oxidation process that contributes additional complexity to the mechanistic study. Indeed, controversies concerning either the initial reaction site or the mechanism for the HEH oxidation processes are frequently found in the literature.[8]

In the present study, ring substituted ethyl α-cyanocinnamates (**1**) and benzylidenemalononitriles (**2**) were studied as oxidants to probe the possible mechanism of aromatization of HEH under thermal conditions. Here we present kinetic and thermodynamic evidence to show that the oxidation of HEH by **1** and **2** most likely occurs by direct hydride transfer from the 4-position of HEH followed by proton loss from the 1-position.

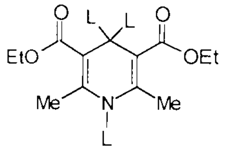

HEH

L=H, D

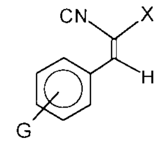

X = -CO$_2$Et (**1**), -CN (**2**)

G: *p*-OCH$_3$ (a), *p*-CH$_3$ (b), *p*-H (c), *p*-Cl (d), *m*-F (e), *p*-Cf$_3$ (f),*p*-CN (g)

Results and discussion

Products of the reductions of ethyl α-cyanocinnamate and benzylidenemalononitrile by HEH

Reaction of Hantzsch 1,4-dihydropyridine (HEH) with **1** or **2** in dry acetonitrile at room temperature proceeded very efficiently, giving redox products in quantitative yield. Both the ^{1}H NMR and mass spectra of the crude products indicated that the C=C double bond in **1** or **2** had been reduced and that two hydrogens in HEH had been eliminated to form a Hantzsch pyridine [eqn. (1)]. The reaction conditions and yields are summarized in Table 1, and demonstrate a simple and highly efficient reaction, which suggests a potential for synthetic applications.

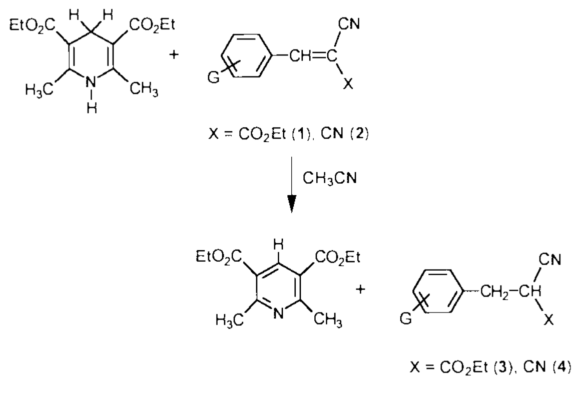

(1)

DOI: 10.1039/b003404p

Table 1 Product yields of the reaction of HEH with **1** and **2** [eqn. (1)] in acetonitrile and the reduction potentials of **1** and **2**

Substrate	Time/h	T/°C	Yield (%)[a]	E_{red}/V *vs.* Fc^+/Fc[b]
1				
G = p-CH_3 (b)	24	rt	95	−1.263
p-CH_3 (b)	24	rt	98	−1.255
p-H (c)	24	rt	94	−1.247
p-Cl (d)	24	rt	96	−1.262
m-F(e)	24	rt	95	−1.260
p-CF_3 (f)	22	rt	96	−1.243
p-CN (g)	22	rt	97	−1.253
2				
G = p-OCH_3 (a)	17	rt	92	−1.335
p-CH_3 (b)	17	rt	95	−1.345
p-H (c)	17	rt	94	−1.275
p-Cl (d)	17	rt	93	−1.289
m-F (e)	17	rt	96	−1.261
p-CF_3 (f)	15	rt	95	−1.229
p-CN (g)	15	rt	94	−1.243

[a] Isolated yield of reduced products of **1** and **2**. [b] Measured by cyclic voltametry (CV) in CH_3CN at 25 °C; error = ± 0.005 V.

The site of hydrogen transfer was determined by ^1H NMR and MS using HEH-4,4-d_2 instead of HEH in the reaction. One deuterium atom was incorporated into the reduced products and was found to be located at the benzylic carbon in **3** and **4**. As an example, the reaction of HEH-4,4-d_2 with **2c** gave **4c**-d_1; in the ^1H NMR spectrum, the integral area of the resonance due to the benzyl proton at 3.32 ppm was one half of that of the corresponding proton in **4c**. Also the triplet at 3.95 ppm for the tertiary hydrogen in **4c** appeared as a doublet in **4c**-d_1. Furthermore, the MS of **4c**-d_1 showed peaks at $m/z = 157$ (15) and 92 (100) for the molecular and the benzyl ions, respectively (Scheme 1). These results unambiguously confirm that the deuterium atom is located at the benzylic position, and, in turn, demonstrate the direction of hydrogen transfer from HEH to **1** and **2** (Scheme 2).

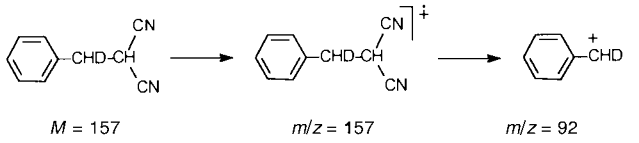

Scheme 1

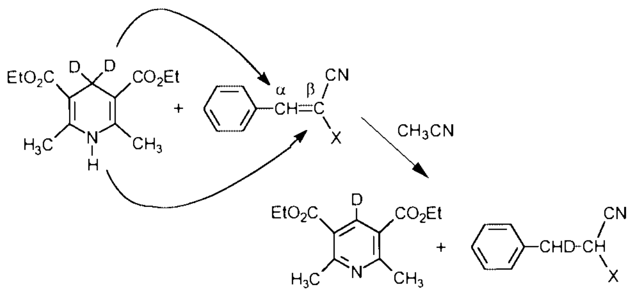

Scheme 2

Kinetics and deuterium isotope effect

The rates of the reaction of HEH (or HEH-4,4-d_2, HEH-N-d) with 40-fold or more excess of **1** and **2** were measured in acetonitrile at 25 °C by monitoring the change in absorption of HEH at $\lambda_{max} = 365$ nm (Fig. 1). The pseudo-first-order rate constants (k_{obs}) were calculated by the Guggenheim method and the second-order rate constants (k_2) were derived from the slopes of the plots of k_{obs} *vs.* [**1**] (or [**2**]). The kinetic isotope effects (KIE) determined by the ratio of second-order rate constants for HEH-N-d and HEH-4,4-d_2 with either **1** or **2** are shown in Table 2.

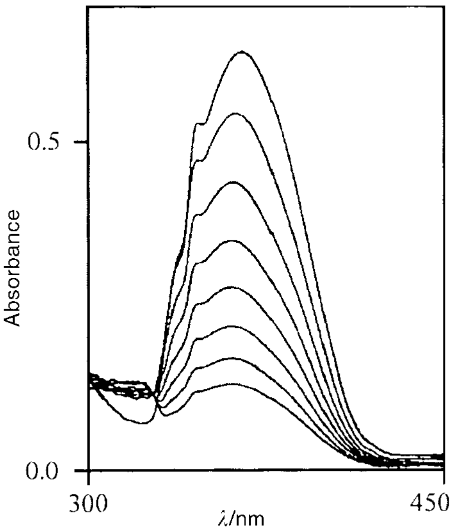

Fig. 1 The absorbance changes at $\lambda_{max} = 365$ nm for the reaction of HEH with **2e** in dry acetonitrile at 25 °C at 1 minute intervals (time increases downwards).

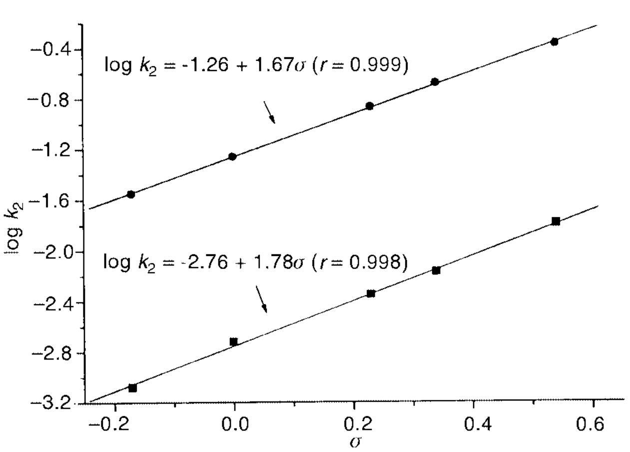

Fig. 2 Correlation of log k_2 *versus* σ constants for the reactions of **1** (■) and **2** (●) with HEH.

The rates of oxidation of HEH by **1** and **2** obey second-order kinetics, showing first-order dependence on each reactant concentration. A Hammett-type free energy analysis of the oxidations of HEH by **1** and **2** shows two excellent linear correlations of log k_2 (from Table 2) with the σ constants of the substituents (Fig. 2) giving ρ values of 1.78 and 1.67 for **1** and **2**, respectively. The positive ρ values indicate the developing negative charge center at the benzylic reaction site of the oxidants (**1** and **2**) in the transition states of the rate-limiting step,[9] which agrees with the mechanism being initiated by either hydride or electron transfer rather than by a neutral hydrogen atom transfer from HEH to **1** and **2**.

The observed kinetic deuterium isotope effects of 1.2–1.3 for the reactions of HEH-N-d with **1** and **2** suggest that N–H bond dissociation is not involved in the rate-limiting step. In contrast, the reaction of HEH-4,4-d_2 with **1** and **2** showed significant kinetic deuterium isotope effects of 5.6–6.0 for **1** and 5.3–5.6 for **2**, which strongly suggests that the C4–H bond dissociation in HEH is the rate-limiting step,[10] and most likely occurs by one-step hydride transfer rather than by one-electron transfer. A reaction mechanism initiated by the ET processes is generally found to possess a much smaller secondary kinetic isotope effect for steric reasons. In addition, the ET process must be

Table 2 Rate constants and kinetic isotope effects (KIE) for the oxidation of HEH, HEH-4,4-d$_2$ and HEH-*N*-d by **1** and **2** in dry CH$_3$CN at 25 °C

Substrates	$k_{obs}/10^{-3}$ min^{-1}	$k_2/10^{-3}$ M^{-1} s^{-1}	$k_2^{4,4\text{-}d_2}/10^{-3}$ M^{-1} s^{-1}	$k_2^{N\text{-}d}/10^{-3}$ M^{-1} s^{-1}	$k_2/k_2^{4,4\text{-}d_2}$ [a]	$k_2/k_2^{N\text{-}d}$ [b]
1						
G = *p*-CH$_3$	0.40	0.83 ± 0.01	0.14 ± 0.02	0.72 ± 0.03	5.98	1.16
p-H	0.91	1.9 ± 0.02	0.32 ± 0.03	1.64 ± 0.02	5.89	1.16
p-Cl	2.2	4.5 ± 0.01	0.78 ± 0.02	3.85 ± 0.02	5.78	1.17
m-F	3.3	6.8 ± 0.02	1.19 ± 0.02	5.82 ± 0.02	5.73	1.17
p-CF$_3$	7.8	16.2 ± 0.02	2.87 ± 0.02	13.7 ± 0.01	5.64	1.18
2						
G = *p*-CH$_3$	13.4	28.2 ± 0.1	5.05 ± 0.3	22.2 ± 0.2	5.58	1.27
p-H	26.3	54.7 ± 0.2	9.95 ± 0.2	43.07 ± 0.2	5.50	1.27
p-Cl	63.8	134.0 ± 0.2	24.8 ± 0.3	104.7 ± 0.1	5.40	1.28
m-F	99.1	208.0 ± 0.2	38.9 ± 0.3	162.5 ± 0.2	5.35	1.28
p-CF$_3$	201.5	423.2 ± 0.2	80.5 ± 0.2	328.1 ± 0.2	5.26	1.29

[a] KIE obtained from the reactions of HEH and HEH-4,4-d$_2$ with **1** or **2**. [b] KIE obtained from the reactions of HEH and HEH-*N*-d with **1** or **2**.

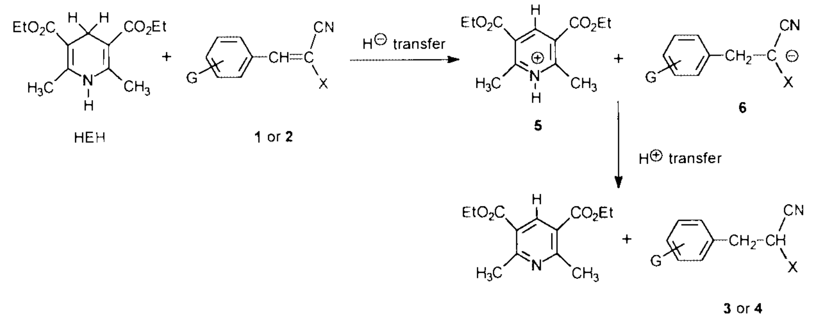

Scheme 3

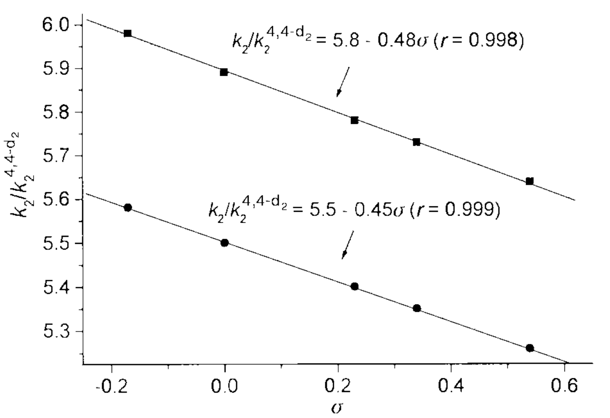

Fig. 3 Plots of KIE ($k_2/k_2^{4,4\text{-}d_2}$) *versus* σ constants for the reactions of **1** (■) and **2** (●) with HEH.

followed by the rate-limiting process of H atom transfer, which cannot have a ρ value of 1.67–1.78.

It is worth pointing out that, in contrast to $k_2/k_2^{N\text{-}d}$, the primary KIE ($k_2/k_2^{4,4\text{-}d_2}$) data shown in Table 2 are substantially influenced by the remote substituents in the benzene ring. This is in agreement with relatively high ρ-values for the reactions, which imply that the benzylic carbon must be close enough to the moving hydride in the transition-state to allow the substituent electronic effect to be effective. Meanwhile, the linear relationship of $k_2/k_2^{4,4\text{-}d_2}$ with respect to the σ-value of the ring substituents (Fig. 3) implies that during the hydride transfer the benzylic C–H bond must have developed substantially in an early stage as the hydride starts to break away from C4–H of HEH. Correlation of $k_2/k_2^{4,4\text{-}d_2}$ against σ are linear for both reaction series (Fig. 3) and have similar slopes (−0.48 and −0.45), suggesting that the two reactions proceed *via* a similar mechanism with a similar transition state. The negative slope indicates the decrease in sensitivity as the substituent changes from electron-donating to electron-withdrawing, and is in accordance with the reactivity–selectivity principle (RSP).[11]

The results described above have allowed us to propose a mechanism (Scheme 3) in which the oxidation of HEH by **1** or **2** is initiated by the rate-limiting step of direct one-step hydride transfer from HEH to **1** or **2** to generate the cation **5** and carbanion **6**, followed by a rapid proton transfer from **5** to **6** to give Hantzsch pyridine and **3** or **4** as the final products.

Activation parameters for the oxidation of HEH with 1 and 2 and free energy changes of one-electron transfer from HEH to 1 and 2

In order to further rule out the possibility of reaction (1) being initiated by electron transfer and to gain a new insight into the transition-state in the rate-limiting reaction step, activation parameters of reaction (1) and free energy changes of electron transfer from HEH to the substrates **1** or **2** were determined. The second-order rate constants of reaction (1) at different temperatures between 20 and 40 °C are given in Table 3. Correlation of ln (k_2/T) *versus* the reciprocal of the absolute temperature ($1/T$) gave a straight line, from which various activation parameters ($\Delta G^{\ddagger}$, $\Delta H^{\ddagger}$, and $\Delta S^{\ddagger}$) were calculated by a least-squares method. The activation parameters of reaction (1) and the free energy changes of one-electron transfer from HEH to **1** and **2** are summarized in Table 4.

From Table 4, it is clear that the free energy changes of one-electron transfer from HEH to **1** or **2** (167–178 kJ mol^{-1}) are about twice as large as the corresponding free energy changes of activation ($\Delta G^{\ddagger}$) of the oxidation of HEH by **1** or **2** (75.0–90.5 kJ mol^{-1}), implying that the oxidation of HEH by **1** or **2** could not be initiated by single electron transfer.

According to the data of $\Delta G^{\ddagger}$ in Table 4, the plot of $\Delta G^{\ddagger}$ *vs.* the σ constants of the substituents gave an excellent straight line with a slope of −9.8 (filled-triangle line in Fig. 4), which is in agreement with the correlation of log k_2 against the σ constants (Fig. 2), again supporting the proposed direct hydride

Table 3 Second-order rate constants k_2 for the oxidation of HEH by **1** and **2** at different temperatures between 20 and 40 °C

	$k_2/10^{-3}$ M^{-1} s^{-1} for the oxidation of HEH by **1**				
T/°C	p-CH$_3$	p-H	p-Cl	m-F	p-CF$_3$
20	0.65 ± 0.02	1.47 ± 0.01	3.38 ± 0.02	5.33 ± 0.02	13.16 ± 0.02
25	0.83 ± 0.01	1.90 ± 0.02	4.50 ± 0.01	6.80 ± 0.02	16.20 ± 0.02
30	1.10 ± 0.02	2.58 ± 0.02	6.16 ± 0.02	9.00 ± 0.02	20.44 ± 0.02
35	1.43 ± 0.02	3.35 ± 0.02	8.15 ± 0.02	11.22 ± 0.02	25.48 ± 0.03
40	1.93 ± 0.03	4.46 ± 0.03	11.55 ± 0.03	14.71 ± 0.03	31.87 ± 0.03
	$k_2/10^{-2}$ M^{-1} s^{-1} for the oxidation of HEH by **2**				
20	2.28 ± 0.02	4.42 ± 0.02	11.08 ± 0.02	17.03 ± 0.02	35.35 ± 0.02
25	2.82 ± 0.01	5.47 ± 0.02	13.40 ± 0.02	20.80 ± 0.02	42.32 ± 0.02
30	3.54 ± 0.02	6.99 ± 0.02	16.53 ± 0.02	25.50 ± 0.02	49.84 ± 0.03
35	4.33 ± 0.02	8.72 ± 0.03	19.59 ± 0.03	30.58 ± 0.04	58.28 ± 0.04
40	5.43 ± 0.03	11.16 ± 0.04	24.22 ± 0.03	37.27 ± 0.04	68.59 ± 0.05

Table 4 Activation parameters of hydride transfer and free energy changes of electron transfer from HEH to **1** or **2**

Substrates	$k_2/10^{-3}$ M^{-1} s^{-1}	$\Delta H^{\ddagger}$/kJ mol^{-1}	$-T\Delta S^{\ddagger a}$/kJ mol^{-1}	$\Delta G^{\ddagger}$/kJ mol^{-1}	$\Delta G(\mathrm{ET})^{b}$/kJ mol^{-1}
1					
G = p-CH$_3$	0.83 ± 0.02	38.5 ± 0.2	51.9 ± 0.2	90.4 ± 0.2	169.7
p-H	1.90 ± 0.01	39.4 ± 0.4	49.0 ± 0.4	88.4 ± 0.4	168.9
p-Cl	4.50 ± 0.02	34.9 ± 0.3	51.4 ± 0.3	86.3 ± 0.3	170.1
m-F	6.80 ± 0.03	35.8 ± 0.4	49.5 ± 0.3	85.3 ± 0.3	170.1
p-CF$_3$	16.2 ± 0.02	31.1 ± 0.4	52.2 ± 0.4	83.3 ± 0.4	168.4
2					
G = p-CH$_3$	28.2 ± 0.01	30.2 ± 0.3	51.6 ± 0.3	81.8 ± 0.3	178.4
p-H	54.7 ± 0.01	32.5 ± 0.4	47.6 ± 0.4	80.1 ± 0.4	171.6
p-Cl	134.0 ± 0.02	27.1 ± 0.4	50.9 ± 0.4	78.0 ± 0.4	173.0
m-F	208.0 ± 0.03	27.35 ± 0.2	49.5 ± 0.2	76.7 ± 0.2	170.3
p-CF$_3$	423.2 ± 0.02	23.1 ± 0.3	51.9 ± 0.3	75.0 ± 0.3	167.2

[a] T = 25 °C. [b] Free energy changes of one-electron transfer from HEH to **1** or **2** were estimated on the basis of relevant redox potentials from Table 1, using E_{ox} (HEH) = 0.508 V (*vs.* Fc$^+$/Fc) from this work.

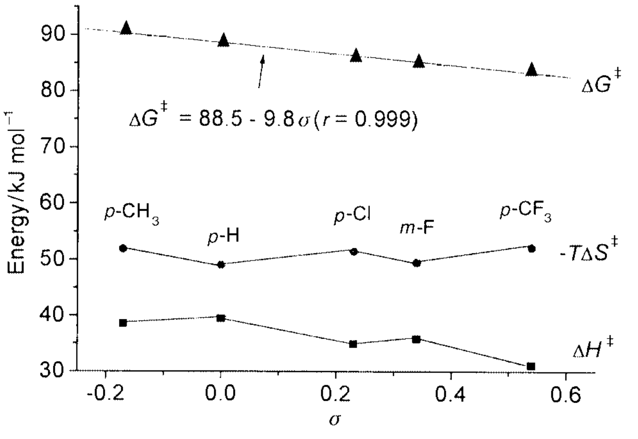

Fig. 4 Plots of $\Delta G^{\ddagger}$(▲), $\Delta H^{\ddagger}$(■), and $-T\Delta S^{\ddagger}$(●) *versus* σ constants for the reactions of **1** with HEH.

transfer mechanism in Scheme 3. Contrary to the plot of $\Delta G^{\ddagger}$, the plots of $\Delta H^{\ddagger}$ and $-T\Delta S^{\ddagger}$ *vs.* the σ constants show two saw-shaped lines rather than straight lines, which indicates that neither of the $\Delta H^{\ddagger}$ and the $-T\Delta S^{\ddagger}$ possesses a linear Hammett relationship with the σ constants. However the two saw-shaped lines are obviously complementary to one other, and combine ($\Delta G^{\ddagger}$) to give an excellent linear relationship with the σ constants.

Comparing the plots of $\Delta H^{\ddagger}$ and $-T\Delta S^{\ddagger}$, it is interesting to note that the $-T\Delta S^{\ddagger}$ values are, generally, larger (in an absolute sense) than the corresponding $\Delta H^{\ddagger}$. This indicates that the NAD(P)H model reactions are likely to be entropy-controlled processes, which, to our knowledge, has not been quantitatively demonstrated in previous NAD(P)H model studies. Examination of the relationship of $\Delta S^{\ddagger}$ with size of the substituents shows that the larger the group, generally, the more negative the $\Delta S^{\ddagger}$, which demonstrates that the transition-state for the hydride transfer from HEH to **1** or **2** is "contacted".

Conclusions

The controversial mechanism for the HEH-modeled NAD(P)H reductions with α,β-unsaturated esters (**1**) and cyanides (**2**) has been clarified by a thorough kinetic and thermodynamic investigation. Evidence collected from the isotopic trace, KIE, activation parameter analyses, and the Hammett-type correlation (LFER) suggests that oxidation of HEH by **1** or **2** to form Hantzsch pyridine and the reduction products (**3** or **4**) proceeds *via* a direct one-step hydride migration from the C4-position of HEH to the benzylic carbon of the substrate, which is then followed by a rapid proton transfer from the N-position of **5** to the intermediate carbanion **6** to form the final products (Scheme 3). This reaction also provides a mild and high-yielding synthetic approach for selectively reducing the C=C double bond in α,β-unsaturated esters and nitriles.

Experimental

Materials and general instruments

Hantzsch ester (HEH) was synthesized by the method of Love and Snader,[12] mp 191.0–191.5 °C. HEH-*N*-d and HEH-4,4-d$_2$ were prepared according to literature procedures.[13] Benzylidenemalononitrile, ethyl α-cyanocinnamate and their derivatives were prepared by condensation of the corresponding aldehydes with malononitrile or with ethyl α-cyanoacetate in the presence of a base.[14] Acetonitrile (AR grade) was refluxed with $KMnO_4$ and K_2CO_3 and redistilled before use. Other reagents were used as received (AR grade). A 4X micro-melting-point apparatus, JEOL FX-90Q NMR spectrometer, ZAB-MS spectrometer and a Hitachi U-3000UV-vis spectrophotometer were used for analytical purposes.

General procedure for the oxidation of HEH by 1 and 2

A mixture of **1** or **2** (0.8 mmol) and HEH (1.6 mmol) in 40 mL de-aerated acetonitrile was left in the dark at room temperature for over 24 h. The solvent was then rotary evaporated and the residue was subjected to column chromatography on silica gel with light petroleum–ethyl acetate as eluant to give the redox products Hantzsch pyridine and **3** or **4** (yield of more than 90%). The structures of **3** and **4** were determined by ^{1}H NMR and mass spectrometry. The data of the representative products **3c** and **4c** are shown below.

Product **3c**: ^{1}H NMR (400 MHz, $CDCl_3$): δ 1.28 (t, $J = 6$ Hz, 3H), 3.27 (m, 2H), 3.74 (m, 1H), 4.26 (q, $J = 6$ Hz, 2H), 7.32 (m, 5H). MS: *m/z* 203 (15), 130 (21), 103 (10), 91 (100), 77 (17), 65 (13), 51 (15), 39 (8). Elemental analysis: $C_{12}H_{12}N$ requires C, 71.29; H, 5.94; N, 6.93. Found: C, 71.18; H, 5.90; N, 7.00%.

Product **4c**: ^{1}H NMR (400 MHz, $CDCl_3$): δ 3.32 (d, $J = 6.84$ Hz, 2H), 3.95 (t, $J = 7.07$ Hz, 1H), 7.41 (m, 5H). Elemental analysis: $C_{10}H_8N_2$ requires C, 76.92; H, 5.13; N, 17.95. Found: C, 76.80; H, 5.16; N, 18.04%.

Kinetic measurements

Kinetic measurements were carried out in acetonitrile using a Hitachi U-3000 spectrophotometer connected to a super-thermostat circulating bath to regulate the temperature of cell compartments. The rates of oxidation of HEH by **1** or **2** were measured at 25 °C by monitoring the changes of absorption of HEH ([HEH] = 0.05 mM) at 365 nm under psuedo-first-order conditions (**1** and **2** in over 40-fold excess). The psuedo-first-order rate constants were then converted to k_2 by linear correlation of psuedo-first-order rate constants against the concentrations of **1** or **2**. The activation parameters were determined by the variations of k_2 against reaction temperatures (20–40 °C).

Redox potentials of 1 (2) and HEH

All electrochemical measurements were carried out in dry CH_3CN solution under argon atmosphere as described previously.[15] n-Bu_4NPF_6 (0.1 M) was employed as the supporting electrolyte. A standard three-electrode assembly consisting of a Pt disc as the working electrode, $AgNO_3$/Ag as reference, and a platinum wire as the counter electrode were used in CV measurements. All sample solutions were 1.5 mM. The ferrocenium/ferrocene redox couple (Fc^+/Fc) was taken as the internal standard. Reproducibility was generally less than 5 mV.

Acknowledgements

This work was made possible by grants from the Natural Science Foundation of China (NSFC Nos. 29972028 and 29702005) and in part from the National Laboratory of Applied Organic Chemistry, Lanzhou University.

References

1 Y. Murakami, J. Kikuchi, Y. Hisaeda and O. Hayashida, *Chem. Rev.*, 1996, **96**, 721.

2 (*a*) B. E. Norcross, P. E. Klinedeinst and E. H. Westheimer, *J. Am. Chem. Soc.*, 1962, **84**, 797; (*b*) S. Fukuzumi, S. Mochizuki and T. Tanaka, *J. Am. Chem. Soc.*, 1989, **111**, 1497; (*c*) D. D. Tanner and A. Kharrat, *J. Am. Chem. Soc.*, 1988, **110**, 2968; M. F. Powell and T. C. Bruice, *J. Am. Chem. Soc.*, 1983, **105**, 7139; (*d*) B. W. Carlson, L. L. Miller, P. Neta and J. Gradkowski, *J. Am. Chem. Soc.*, 1984, **106**, 7233; (*e*) N. Ohno, R. Tamura and A. Kaji, *J. Am. Chem. Soc.*, 1980, **102**, 2851; N. Ohno, R. Tamura and A. Kaji, *J. Am. Chem. Soc.*, 1983, 105, 4017; (*f*) A. Anne, J. Moirou and J. M. Saveant, *J. Am. Chem. Soc.*, 1993, **115**, 10224; (*g*) D. M. Chipman, R. Yaniv and P. Van Eikeren, *J. Am. Chem. Soc.*, 1980, **102**, 3244; (*h*) J. W. Bunting, V. S. F. Chew and G. Chu, *J. Org. Chem.*, 1982, **47**, 2303; J. W. Bunting, V. S. F. Chew and G. Chu, *J. Org. Chem.*, 1982, **47**, 2308.

3 (*a*) X.-Q. Zhu and Y.-C. Liu, *J. Org. Chem.*, 1998, **63**, 2786; (*b*) X.-Q. Zhu, Y.-C. Liu, H.-Y. Wang and W. Wang, *J. Org. Chem.*, 1999, **64**, 8983; (*c*) X.-Q. Zhu, Y. C. Liu, J. Li and H. Y. Wang, *J. Chem. Soc., Perkin Trans. 2*, 1997, 2191; (*d*) J.-P. Cheng, Y. Lu, X.-Q. Zhu and L. J. Mu, *J. Org. Chem.*, 1998, **63**, 6108; (*e*) B. J. Zhao, X.-Q. Zhu, J. Q. He, Z. Z. Xia and J.-P. Cheng, *Tetrahedron Lett.*, 2000, **41**, 257.

4 (*a*) F. Powell, S. C. Wu and T. C. Bruice, *J. Am. Chem. Soc.*, 1984, **106**, 3850; (*b*) B. W. Carlson and L. L. Miller, *J. Am. Chem. Soc.*, 1983, **105**, 7453; (*c*) S. Fukuzumi, S. Koumitsu, K. Hironaka and T. Tanaka, *J Am. Chem. Soc.*, 1987, **109**, 305; (*d*) A. Sinha and T. C. Bruice, *J. Am. Chem. Soc.*, 1984, **106**, 7291; (*e*) C. C. Lai and A. K. Colter, *J. Chem. Soc.*, *Chem. Commun.*, 1980, 1115; (*f*) S. Fukuzumi, Y. Kondo and T. Tanaka, *J. Chem. Soc.*, *Perkin Trans. 2*, 1984, 673; (*g*) S. Fukuzumi, M. Ishikawa and T. Tanaka, *J. Chem. Soc.*, *Perkin Trans. 2*, 1989, 1811.

5 (*a*) M. F. Powell and T. C. Bruice, *J. Am. Chem. Soc.*, 1982, **104**, 5834; (*b*) M. F. Powell and T. C. Bruice, *J. Am. Chem. Soc.*, 1983, **105**, 1014; (*c*) J. W. Verhoeven, W. van Gerresheim, F. M. Martiens and S. M. van der Kerk, *Tetrahedron*, 1986, **42**, 975; (*d*) L. L. Miller and J. R. Valentine, *J. Am. Chem. Soc.*, 1988, **110**, 3982; (*e*) B. W. Carlson and L. L. Miller, *J. Am. Chem. Soc.*, 1985, **107**, 479; (*f*) D. Ostovic, R. M. G. Roberts and M. M. Kreevoy, *J. Am. Chem. Soc.*, 1983, **105**, 7629; (*g*) D. Ostovic, I. S. Lee, R. M. G. Roberts and M. M. Kreevoy, *J. Org. Chem.*, 1985, **50**, 4206.

6 (*a*) S. Yasui and A. Ohno, *Bioorg. Chem.*, 1986, **14**, 70; (*b*) S. Fukuzumi, *Adv. Electron Transfer Chem.*, 1992, **2**, 67; (*c*) D. M. Stout and A. I. Meyers, *Chem. Rev.*, 1982, **82**, 223.

7 (*a*) F. Bossert, W. Vater and E. Wehinger, *Angew. Chem.*, *Int. Ed. Engl.*, 1981, **20**, 762; (*b*) X. Y. Wei, A. Ruttedge and D. J. Triggle, *J. Mol. Pharmacol.*, 1989, **35**, 541; (*c*) M. F. Gordeev, D. V. Patel and E. M. Gordon, *J. Org. Chem.*, 1996, **61**, 924.

8 X.-Q. Zhu, Y.-C. Liu and J.-P. Cheng, *J. Org. Chem.*, 1999, **64**, 8980.

9 N. S. Isaacs, *Physical Organic Chemistry*, 1st edn, John Wiley & Sons; New York, 1987, ch. 4.

10 N. S. Isaacs, *Physical Organic Chemistry*, 1st edn, John Wiley & Sons; New York, 1987, ch. 6.

11 M. W. Schmidt, K. K. Baldrige, J. A. Boatz, S. T. Elbert, M. S. Gordon, J. H. Jensen, S. Koseki, N. Matsunnaga, K. A. Nguyen, S. J. Su, T. L. Windus, M. DuPuis and J. A. Montgomery, *J. Comput. Chem.*, 1993, **14**, 1347.

12 B. Love and K. M. Snader, *J. Org. Chem.*, 1965, **30**, 1914.

13 (*a*) A. Singer and M. McElvain, *Org. Synth.*, 1934, **14**, 30; (*b*) B. E. Noecross, G. Clement and M. J. Weinstein, *Educ. Chem.*, 1969, **46**, 695; (*c*) B. E. Norcross, P. E. Klinedinst and E. H. Westheimer, *J. Am. Chem. Soc.*, 1962, **84**, 792.

14 J. Zablicky, *J. Chem. Soc.*, 1961, 686.

15 X.-Q. Zhu, M. Xian, K. Wang and J.-P. Cheng, *J. Org. Chem.*, 1999, **64**, 4187.